
APISERVE: Efficient API Support for Large-Language Model Inferencing

Reyna Abhyankar* Zijian He* Vikranth Srivatsa Hao Zhang Yiying Zhang

University of California, San Diego

Abstract

Large language models are increasingly integrated with external tools and APIs like ChatGPT plugins to extend their capability beyond language-centric tasks. However, today’s LLM inference systems are designed for standalone LLMs. They treat API calls as new requests, causing unnecessary recomputation of already computed contexts, which accounts for 37-40% of total model forwarding time. This paper presents APISERVE, the first LLM inference framework targeting API-augmented LLMs. APISERVE minimizes the GPU resource waste caused by API calls and dedicates saved memory for serving more requests. APISERVE improves the overall serving throughput by $1.6\times$ and completes $2\times$ more requests per second compared to the state-of-the-art LLM inference systems.

1 Introduction

Large language models (LLMs) (OpenAI et al., 2023; Touvron et al., 2023) have shown immense potential in various applications, such as natural language understanding and content generation. Nonetheless, LLMs alone can only generate text. To extend LLMs’ capabilities to handle more diverse and open-ended tasks, a recent trend is to augment LLMs with external tools (Parisi et al., 2022; Schick et al., 2023; Hao et al., 2023; Mialon et al., 2023) such as arithmetic calculation (Hao et al., 2023) and virtual-environment interaction (Shridhar et al., 2020), or interact with humans and the other environments in real-time, such as chatgpt-plugins. (OpenAI, 2023). More generally, we can view the use of tools and the interaction with humans or the environment all as LLMs *calling APIs*.

APIs have unique properties that bring new problems to LLM inference systems. First, API calls intercept or *pre-empt* regular LLM decoding, *i.e.*, when an API call is made,

the normal decoding phase is paused and can only resume when the API returns. Second, an API’s execution time varies drastically across API types and requests. For example, a calculator API finishes in less than 1 ms, yet it may take humans more than 1 minute to digest and type a subsequent chat prompt. The uncertain API execution time complicates request scheduling. Third, unlike regular requests, the context (*i.e.*, KV caches) cannot be used for a paused request during API calls but will be needed upon API return. It is unclear how to handle *temporarily unused context*. Adding to the complexity is the high variation in context length and API execution time across requests.

Unfortunately, existing LLM inference systems (Kwon et al., 2023; Yu et al., 2022; Li et al., 2023; Aminabadi et al., 2022; NVIDIA, 2023; Agrawal et al., 2023) fall short in serving LLMs with API calls. They typically interpret an API call within a request as a termination signal – they conclude the ongoing request at the point of an API call, discard its context, relegate the task to the API provider, and subsequently re-initiate a new request upon receiving the API’s output. Consequently, when a request frequently invokes API calls, for each API call, the initial prompt and all tokens generated before the API call are formed as a new request submitted to the inference system, causing substantial recomputation of keys and values for all previously processed tokens. This recomputation wastes GPU resources, which could otherwise be used to serve new requests.

In contrast to the aforementioned API handling approach (which we refer to as *Discard*), an alternative approach is to preserve a request’s context during the API call and resume the request when the API call returns. This approach, which we call *Preserve*, avoids recomputation but occupies GPU memory for the entire API execution time. This GPU memory could accommodate other requests’ context and increase overall throughput (Kwon et al., 2023).

To avoid recomputation and memory preservation, another possible approach to handle APIs is to swap contexts to CPU memory when an API is called (we call it *Swap*). Although *Swap* avoids recomputation and GPU memory wastage, with limited GPU-CPU link bandwidth, foreground tasks (normal forwarding) could be bottlenecked by

*Equal contribution

waiting for swapping to finish. The GPU memory could be used for processing more requests.

How should an LLM inference system efficiently support API calls? To answer this question, we first study the computational patterns of LLM augmented with six typical types of APIs: arithmetic, question-and-answer, virtual environment, chatbot, image generation, and text-to-speech transformation. We then evaluate how well the state-of-the-art LLM inference system, vLLM (Kwon et al., 2023) (which performs `Discard`), and the two possible extensions (`Preserve` and `Swap`) perform on these APIs.

Based on our findings, we propose APISERVE, the *first* LLM inference framework targeting API-augmented LLMs. The core idea of APISERVE, which we call *min-waste preemption*, is to minimize GPU memory waste caused by API calls so that the same amount of GPU resources can be used to serve more requests. To this end, APISERVE incorporates three contributions. First, we deduce three waste-calculation equations to quantify the GPU memory waste of `Discard`, `Preserve`, and `Swap`.

Second, we improve individual preemption techniques to reduce or eliminate their memory waste. For `Swap`, we propose swap pipelining, which overlaps swapping and foreground computation in a model-layer-by-layer manner. Additionally, we split the swapping of a sequence into multiple iterations so that each iteration’s swap needs stays within what the GPU-CPU link can sustain (*i.e.*, a swap budget). As a result, APISERVE completely eliminates GPU memory waste of `Swap`. For `Discard`, we observe that certain GPU processing capacity is unused by running requests at each iteration because of the imbalanced memory/computation requirements of decoding. We utilize this unused capacity for recomputation. We split requests’ contexts into chunks, each small enough to fit within the unused capacity and recomputed in one iteration.

Finally, APISERVE dynamically chooses the preemption and resuming strategies within and across requests to minimize overall GPU memory waste while ensuring fairness. For preemption scheduling, we sort API-preempted requests by their potential memory waste and assign the swap budget to requests with the highest potential waste. For the remaining requests, we discard or preserve their context based on the waste comparison. For resuming scheduling, we assign the swap budget to swapped-out requests with the earliest original arrival times (FCFS). We also schedule discarded requests, preserved requests, and non-API waiting requests according to FCFS, adding requests until the GPU’s processing capacity is reached.

We implement APISERVE on top of vLLM (Kwon et al., 2023), a state-of-the-art LLM inference system. We eval-

An iteration is a single model forwarding pass.

uate APISERVE, vLLM (`Discard`), `Preserve`, and `Swap` on A100 GPUs using two LLMs (GPT-J-6B (Wang & Komatsuzaki, 2021) and Vicuña-13B (Chiang et al., 2023)) and the six API types we study. Overall, APISERVE sustains $1.6\times$ higher serving load than vLLM while maintaining similar latency per token generation. APISERVE also achieves over $2\times$ more completed requests per second. We will open source APISERVE soon.

2 API-Augmented LLMs

This section first discusses popular API-augmented LLM frameworks and then presents properties of typical APIs from our empirical study.

2.1 API-Augmented LLM Frameworks

To extend LLMs’ ability to undertake more types of tasks, various approaches have been proposed to *augment* an LLM with tool, or API, uses. Below, we briefly describe typical API uses in two broad categories.

The first type of APIs are non-LLM tools called during the decoding phase of an LLM, usually aimed to extend the type of tasks the LLM can handle. These APIs range from simple tools like calculator (Wolfram, 2023) and calendar to real-world interactions like information retrieval (Baeza-Yates et al., 1999) and restaurant reservation (OpenTable, 2023). Additionally, an API can invoke another machine-learning model such as translation (Costa-jussà et al., 2022) and question-answering (QA) (Izacard et al., 2022). An LLM is usually fine-tuned to generate appropriate API calls automatically during the decoding phase, with frameworks like TaLM (Parisi et al., 2022), ToolkgenGPT (Hao et al., 2023), and Toolformer (Schick et al., 2023).

The second type augments a single triggering of an LLM by making a *sequence* of calls to the same LLM or to other tools. For example, to continuously interact with a human, a chatbot can take rounds of back-and-forth chats by calling an LLM at each step and maintaining a chat history (Greyling, 2023). Another popular use case is decomposing a complex task into multiple steps. For example, Chain-of-Thoughts (Wei et al., 2022; Zhang et al., 2022) breaks one request into a chain of “thought” steps, each being a new prompt to an LLM that continues the history of thoughts. Similarly, ReAct (Yao et al., 2022) uses a chain of reasoning and action to accomplish complex tasks. To assist users in expressing such augmented LLM usages, LangChain (Chase, 2022), Gorilla (Patil et al., 2023), and SGLang (Zheng et al., 2023b) provide programming models for users to trigger LLMs or tools in a task flow.

Type	Exec Time (sec)	Num API Calls	Context Len
Math	(9e-5, 6e-5)	(3.75, 1.3)	(1422, 738)
QA	(0.69, 0.17)	(2.52, 1.73)	(1846, 428)
VE	(0.09, 0.014)	(28.18, 15.2)	(2185, 115)
Chatbot	(28.6, 15.6)*	(4.45, 1.96)	(753, 703)
Image	(20.03, 7.8)†	(6.91, 3.93)*	(1247, 792)
TTS	(17.24, 7.6)†	(6.91, 3.93)*	(1251, 792)

Table 1: **API Properties** Each cell shows (mean, variance) of API calls of the type. * estimated behavior. † partially estimated.

2.2 API Calls and Their Properties

To understand LLM APIs and design inference systems for them, we first examine a set of representative APIs, including arithmetic (math), question-and-answer (QA), virtual environment (VE), chatbot, image generation, and text-to-speech (TTS), to answer three key questions: 1) how long does an API call take? 2) how many API calls are generated for a request? and 3) what is the context length when an API call is made? Table 1 summarizes our results with averages and variations. We leave other metrics like API returned token length, detailed CDF distributions, and our evaluation methodology to the Appendix.

Arithmetic (Math). To solve complex math problems, an LLM can be augmented to deconstruct the problem and call a calculator API step-by-step. We evaluate this use case with the GSM8K-XL (Hao et al., 2023) dataset, which contains 8.5K high-quality grade school math problems. As expected, the calculator API’s execution times are short, an average of 0.2 ms. It has a fairly large context length when APIs are called since we must prompt the LLM with demonstrations of solving problems step-by-step.

Knowledge-based question and answer (QA). To allow pre-trained LLMs to access wider sets of knowledge, one can augment the LLM to call knowledge-based QA APIs that retrieve information from a rich dataset. We use the Multihop QA Wikipedia (Yang et al., 2018) dataset to evaluate this API use. These APIs, while having longer context lengths for questions, provide relatively quick yet variable execution times due to the non-deterministic network communication latency with Wikipedia.

Virtual Environment (VE). An LLM can be augmented to interact with virtual environments and accomplish complex tasks by performing gradual steps (Gu et al., 2022; Huang et al., 2022; Hu et al., 2023). To evaluate VE APIs, we use the ALFWorld dataset (Shridhar et al., 2020), an interactive environment that aligns text descriptions and commands with a physically embodied robotic simulation. This VE API has a short and stable execution time due to a locally executed and embodied text-based environment. The context length is long due to the instructions needed to prompt the LLM to understand VE action sequences.

Chatbot. A popular task for LLMs is a chatbot, which interacts with human with a sequence of chats. Here, we

view human responses as an API, as the time that humans use to respond essentially “leaves,” or *preempts*, regular LLM processing, but the chat history should be kept as a context for following chats. To evaluate chatbots, we use the ShareGPT dataset (Zheng et al., 2023a), which contains crowd-sourced real-user ChatGPT conversations. We estimate human response time (*i.e.*, the API execution time) as the summation of human scanning time (Brysbart, 2019) of the previous chat response and typing time (Ma et al., 2015) of the next prompt. The context lengths vary greatly due to the variety of human chat sequences. Accordingly, the Chatbot API execution time also has a high variance.

Image Generation. An LLM can be augmented to generate a sequence of images when a human gradually refines features through multiple prompts (*e.g.*, adding details to a face depiction). This involves two APIs: one for image generation and another for receiving user prompts. The latter API type is similar to Chatbot’s. To understand this use case, we use ChatGPT to create a dataset by generating a series of image-generation prompts, each triggering a call to the Stable Diffusion model (Rombach et al., 2021). The execution time of the image generation API has high variation due to variations in executing a diffusion model and the variation in human response time. The average context length is shorter than the Chat API due to smaller input prompts to the diffusion API.

Text-To-Speech (TTS). As demonstrated by the ChatGPT Whisper API support (Brockman et al., 2023), TTS can be integrated with an LLM to communicate with a human. Similar to our image-generation dataset, we use ChatGPT to generate a series of prompts, each triggering an API call to the Bark TTS model (AI, 2023). Similar to image generation, we estimate the human response time but measure actual TTS execution time. TTS’s behavior also has high variation in API execution time due to variations in model execution time and user response time.

Summary and Insights. Overall, we find API execution time to be highly dependent on API types and exhibit a clear difference between short-running (Math, QA, VE) and long-running (Chatbot, Image, TTS) ones. The short-running APIs are fully automated with no human interaction. Most of them also exhibit small variations (except for QA, which interacts with the network). APIs that involve human interaction and/or calling another large model are long-running with high variations. The short/long execution times and their variation imply that no single API preemption strategy is universally applicable, but an inference system could utilize API type as a hint for execution time. Context lengths for all the APIs are large, implying potential high GPU memory wasted. Context lengths also see high variation, complicating the handling of them at the run time.

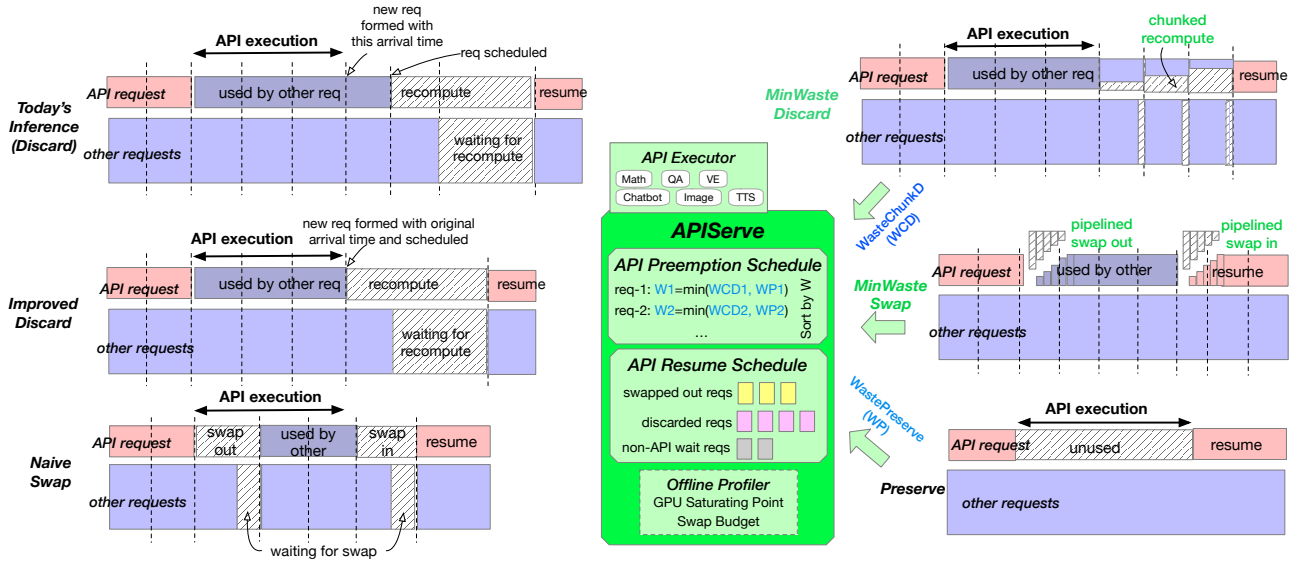


Figure 1: **APISERVE and Alternative Approaches.** Vertical: GPU resources occupied or wasted by API and other requests. Horizontal: timeline divided by iterations (dotted vertical lines). Hatch parts represent memory waste. APISERVE adaptively combines preserve, our optimized discard, and our optimized swap. All green parts represent APISERVE’s techniques.

3 Existing LLM Inference Systems

This section discusses related works in existing LLM inference systems and why simple extensions to them are insufficient for API handling, as shown in Figure 1.

3.1 LLM Inference Systems

Recent years have seen the rise of inference systems that are designed specifically for LLMs. Unlike APISERVE, none of the existing inference systems are designed for handling APIs, and all suffer from unoptimized performance, as we will show in Section 3.2.

Some of them aim to improve overall inference throughput with better scheduling strategies. For example, Orca (Yu et al., 2022) proposes iteration-level scheduling where, at the end of each model forward pass, Orca’s scheduler is invoked to form a new batch for the next forward pass. Such iteration-level scheduling strategies improve GPU utilization, resulting in higher inference throughput. APISERVE also adopts iteration-level scheduling but with a unique and new scheduling strategy — at each iteration, APISERVE makes a decision for requests calling and returning from APIs in a manner that minimizes GPU memory wastage based on their API call properties. Apart from FCFS which Orca and others use, alternative request scheduling policies such as multi-level feedback queue in FastServe (Wu et al., 2023) have been proposed. We leave the comparison of these scheduling policies to future work.

Another optimization target is GPU memory usage. vLLM (Kwon et al., 2023) proposes the concept of paged attention, where KV caches are treated as virtual mem-

ory that can map to non-contiguous physical GPU memory. Because of the flexibility in virtual memory, vLLM achieves better utilization of GPU memory, thereby improving overall inference performance. APISERVE also utilizes paged attention to efficiently use GPU physical memory. Unlike vLLM, which is agnostic to APIs, APISERVE adaptively preserves, discards, or swaps KV cache of API-preempted requests to minimize memory waste. Other memory-efficient techniques, such as prefix sharing in SGLang (Zheng et al., 2023b), are orthogonal and can potentially be added to APISERVE.

Yet another set of LLM inference systems focuses on the imbalanced computation needs between the prefill and decoding stages. Sarathi (Agrawal et al., 2023) is a system that proposes the technique of chunked prefill, which splits prompt tokens into chunks, each merged with other decoding requests to form one iteration’s batch. APISERVE’s chunking splits sequences for recomputation and swapping to fully utilize GPU and GPU-CPU-link resources while minimizing memory waste. Other proposals on prefill-decoding optimization like DistServe (Zhong et al., 2024) are orthogonal and can potentially be added to APISERVE.

3.2 Limitations of Inference Systems and Extensions

We now qualitatively and quantitatively analyze the limitations of existing LLM inference systems and naive extensions to them for API support. We quantify the impact of these approaches on serving speed with our proposed GPU memory waste calculation.

Discard-based approaches. Today’s LLM inference systems are not designed for APIs. To use them for APIs,

one would need to treat the API call preemption as the end of the request and re-initiate a request when the API returns. With today’s inference systems using the FCFS scheduling policy, they would schedule these re-initiated requests at the end of the waiting queue and starve API requests. An easy fix to this scheduling problem is using an API request’s original arrival time when re-inserting the resumed request to the waiting queue (we call this scheme `ImprovedDiscard`).

`Discard` and `ImprovedDiscard` both require the re-computation of all context tokens and incur GPU memory waste from two aspects. First, the recomputing itself consumes memory not used for producing any new tokens. Assuming the context for request i when calling API j has C_i^j tokens, each token’s KV value occupies M memory, and recomputation takes $T_{fwd}(C_i^j)$ time, where T_{fwd} is a mapping from the number of scheduled tokens in a batch to the execution time of that iteration. Then the memory wasted for the recomputation is $T_{fwd}(C_i^j) \times C_i^j \times M$. Second, recomputing the context increases iteration time, as an iteration now needs to finish all the recomputation alongside model forwarding of other running requests. The memory occupied by the other running requests is wasted during the additional iteration time, $T_{fwd}(C_i^j)$. Thus, the memory waste for this reason is $T_{fwd}(C_i^j) \times C_{other} \times M$, where C_{other} is the sum of the contexts of other requests. The total memory waste for `Discard` and `ImprovedDiscard` is:

$$\begin{aligned} \text{WasteDiscard}_i^j &= T_{fwd}(C_i^j) \times C_i^j \times M \\ &+ T_{fwd}(C_i^j) \times C_{other} \times M \end{aligned} \quad (1)$$

In practice, our evaluation shows that `Discard` incurs a GPU resource wastage (GB*min) of 27%, and 37-40% of the total model forwarding time is spent on recomputation with a mixed workload containing all six APIs in §2.

Preserve-based approach. Instead of discarding, one could preserve the context of a request when its API call executes. This `Preserve` strategy avoids recomputation cost and can immediately resume a request when its API call returns. However, the preserved context wastes GPU memory for the entire API execution time. The preserve waste P_i^j for request i when calling API j is the API execution time, T^j , multiplied by the amount of GPU memory held by the request’s context.

$$\text{WastePreserve}_i^j = T_{API}^j \times C_i \times M \quad (2)$$

Our measured GPU memory waste with real APIs is surprisingly high: nearly half of the GPU memory is occupied by interrupted requests for more than 60% of the time.

Swap-based approach. To avoid recomputation over-

head in `Discard` and memory waste in `Preserve`, one potential way is to swap all context data from GPU to CPU memory when an API call happens and swap it back to GPU upon the API’s return. The straightforward implementation of `Swap` performs swapping in a synchronous manner by launching CUDA kernels for the movement, moving out/in the data, and then letting computation utilize the memory space. Swapping can take an extremely long time with huge contexts because of the volume of data to be moved and the kernels to be launched. To elaborate on the latter, multiple kernels need to be launched, each for a discontinuous physical memory region. With `PagedAttention` (Kwon et al., 2023), the context of an API request can scatter across physical memory regions, causing high kernel launching time.

Similar to `Discard`, `Swap` incurs memory waste from two sources. First, the memory space being swapped is wasted during the swap time, accounting for $T_{swap}(C_i^j) \times C_i^j \times M$, where T_{swap} is a mapping from the the number of tokens to swap to the corresponding swapping latency. Second, `Swap` could increase the iteration time, causing all running requests to wait for the swapping to finish and do nothing. This waste is $T_{swap}(C_i^j) \times C_{other} \times M$. The total waste doubles to account for swapping in and out:

$$\text{WasteSwap}_i^j = 2 \times T_{swap}(C_i^j) \times C_{batch} \times M \quad (3)$$

Our evaluation shows that `Swap` wastes 26% GPU resources, and over 25% of the total execution time is spent on waiting for swap with the mixed workload.

4 APISERVE

This section presents APISERVE and its min-waste pre-emption designs, also illustrated in Figure 1.

4.1 Swap Pipelining and Chunking

We discuss how APISERVE avoids swap memory waste.

Swap pipelining and overlapping.

`Swap` performs swapping in a serial manner and blocks foreground computation for the entire swap time. To mitigate this problem, we propose to perform swapping in a pipelined manner and in the background. Specifically, APISERVE views each model layer’s swapping as one pipeline stage and pipelines kernel launching, data movement, and foreground model forwarding. For example, when we launch the swap kernel for layer $i + 2$, we move the context for layer $i + 1$, and layer i ’s context has been freed and used for normal forwarding.

Swap chunking. To further reduce memory waste, we propose to chunk swap out and swap in across multiple it-

erations so that in each iteration, the swap latency can be hidden by overlapping it with model forwarding. We obtain T_{fwd} through offline profiling and calculate T_{swap} based on the swapping bandwidth and the per-token memory requirements M . At iteration i with batch size B_i , we set $T_{swap}(N_i) = T_{fwd}(B_i)$ and solve for N_i , which we call the *swap limit*. This overlaps swapping with model forwarding.

Determining swap-in and swap-out budget. At every iteration, there can be tokens waiting to be swapped out and swapped in. APISERVE determines how much bandwidth to give to swap out and to swap in at each iteration by maximizing inference throughput (*i.e.*, the number of tokens that can be added to an iteration’s processing) while guaranteeing the following criteria: 1) the total amount of swap-in and swap-out tokens should be at most N_i ; 2) the amount of swapped-out memory should not exceed the amount of free CPU memory plus the swapped-in memory; and 3) the amount of swapped-in memory and memory for newly scheduled tokens (*i.e.*, our maximizing target) should not exceed the amount of swapped-out memory and free GPU memory. We use the obtained swap-in and swap-out budget when deciding per-request preemption schedule in §4.3.

4.2 Recomputation Chunking

Unlike *Swap*, which consumes GPU-CPU-link bandwidth and can be hidden from foreground GPU tasks, the recomputation of discarded tokens requires GPU resources that cannot be avoided. However, we make a key observation that decoding and recomputation have complimentary resource requirements, with decoding requiring less GPU core resources (for one query token) than recomputation (queries for the entire context length) for the same amount of memory. Thus, a batch of decoding requests usually cannot fill all GPU cores before running out of GPU memory. Mixing decoding and recomputation requests can increase GPU core utilization while staying within the GPU memory boundary. The main challenge to solve is how much recomputation to mix with decoding.

Discard and *ImprovedDiscard* impose the recomputation of an entire request in one iteration. Recomputation of long context can easily add too much computation burden than what a GPU can handle, causing significantly increased iteration time. As a result, long $T_{fwd}(C_i^j)$ causes huge *WasteDiscard* in Equation 1.

To mitigate this issue, we propose an adaptive technique that separates the recomputation of a context sequence into chunks, each added to one iteration without going beyond what the GPU can sustain. We observe that for a given model architecture, the number of query tokens that all the GPU cores can process in parallel is limited and fixed. We call this number the GPU *saturation point*, S , expressed as

a number of query tokens. Processing more query tokens beyond S increases iteration time without improving serving throughput. APISERVE obtains S from offline profiling and sets the chunk size as S minus the running group size.

The memory waste of our chunked recomputation mechanism can be calculated in two parts, similar to Equation 1. For the recomputation itself, we add one chunk of memory waste per iteration that lasts until all chunks have been recomputed, which essentially cuts the waste of *Discard*’s all-recomputation-at-once scheme by half (*i.e.*, $T_{fwd}(C_i^j) \times C_i^j \times M/2$), as illustrated in Figure 1. The second part of waste comes from other requests’ occupied memory during recomputation-added iteration time. This waste amounts to $n \times T_{fwd}(\frac{C_i^j}{n}) \times C_{other} \times M$, where n is the number of iterations to finish recomputing the request and $T_{fwd}(\frac{C_i^j}{n})$ is the per-chunk added iteration time. Adding these two parts, we have the total recomputation memory waste of chunked recomputation as

$$\begin{aligned} \text{WasteChunkD}_i^j &= \frac{T_{fwd}(C_i^j) \times C_i^j \times M}{2} \\ &+ n \times T_{fwd}(\frac{C_i^j}{n}) \times C_{other} \times M \end{aligned} \quad (4)$$

Compared to Equation 1, the left term (recomputation itself) cuts the corresponding term of *Discard* by half, and the right term (other requests) is no larger than the right term of *Discard* because $n \times T_{fwd}(\frac{C_i^j}{n}) \leq T_{fwd}(C_i^j)$. Meanwhile, APISERVE increases GPU core utilization and further improves overall serving throughput.

4.3 Inter-Request Action Decision

Scheduling API-preempted requests. We now discuss how APISERVE schedules API-preempted requests using a hybrid of *preserve*, our improved *swap*, and our improved *discard* when considering multiple requests together. First, for each request i preempted by API j , we calculate its memory waste as the min of *WastePreserve* (Equation 2) and *WasteChunkDiscard* (Equation 4):

$$\text{Waste}_i^j = \min(\text{WastePreserve}_i^j, \text{WasteChunkD}_i^j) \quad (5)$$

Next, we sort all API-preempted requests in descending order of their memory waste. We swap out context from these requests according to this order until we run out of swap-out budget. For the remaining API-preempted requests, we *preserve* or *discard* their remaining context based on its decision from Equation 5 (*i.e.* to *preserve* or *discard*).

Scheduling API-returned and other waiting requests.

At the beginning of each iteration, APISERVE determines what requests to insert into the batch for the iteration. To facilitate this decision, APISERVE maintains three queues:

a running queue containing currently running requests in the system, a swap queue containing requests that have been swapped out and have returned from API calls, and a waiting queue. The waiting queue contains discarded requests that have returned from API calls, new requests received by APISERVE that have never been served, and previously running requests that have been descheduled due to lack of GPU resources. The latter two types are the same as today’s inference systems. Each queue is sorted by its requests’ original arrival times.

At each iteration, we choose requests from the waiting queue in the FCFS (First-Come First-Serve) order until the GPU saturation point is reached; FCFS ensures fairness and avoids starvation. Requests chosen can be any of the three aforementioned waiting types. If it is a discarded request, the iteration will perform the recomputation of the scheduled number of tokens. If this request has only been partially recomputed, it remains in the wait queue with the remaining tokens. At each iteration, we also choose requests from the swap queue in the FCFS order until the swap-in budget is reached. We maintain and schedule a separate swap queue because the swap-in budget is additional to GPU resources and should always be utilized by API requests as much as the budget allows.

4.4 API Execution Time Estimation

The calculation of memory waste for preserving context (Equation 2) requires having a value for the API execution time. For API types with large variations in execution times and for API types not profiled offline, we propose a dynamic estimation method by setting $\hat{T}_{API} = t_{now} - t_{call}$ where t_{now} is the current time updated at each iteration and t_{call} is the time when the API was invoked. Effectively, the longer a request is paused, the larger API time it gets assigned. Our evaluation shows that APISERVE using this estimation method achieves 93% of the performance compared with using an oracle for API execution time.

5 Evaluation Results

We implement APISERVE on top of vLLM and reuse its PagedAttention technique. We compare APISERVE to vanilla vLLM, ImprovedDiscard, Preserve, and Swap, as discussed in §3.2. To evaluate APISERVE and the baselines, we augment the 6B-parameter GPT-J model (Wang & Komatsuzaki, 2021) and the 13B Vicuna model (Chiang et al., 2023) with APIs presented in §2. We run augmented GPT-J on one NVIDIA A100 GPU on an AWS p4d instance. For Vicuna, we use two environments: running on a single A100 GPU and distributed on two A100 GPUs in one p4d instance. To mimic real-world serving scenarios that often receive different types of requests, we use a request dataset that merges the six API types pre-

sented in §2 by uniformly sampling requests from them.

5.1 End-to-End Performance

We first compare the end-to-end performance of APISERVE and the baselines. Following recent LLM inference research papers (Kwon et al., 2023; Yu et al., 2022), we first report the serving throughput as normalized latency (*i.e.*, the median of every request’s end-to-end latency divided by its output length) when varying request load (number of requests arrived per second). Under the same normalized latency, a higher-throughput system should sustain a higher request rate. Apart from normalized latency, we also report the number of finished requests per second. Figure 2 and Figure 3 show these results for APISERVE and the baselines on the 6B and 13B models. For 13B, we report both a single GPU and two GPU executions.

6B model results. APISERVE outperforms baselines across all metrics. APISERVE sustains up to $1.6\times$ higher request arrival rate at the same normalized latency on the 6B model compared to vLLM. Under the same request rate, APISERVE’s normalized latency is $1.9\times$ - $5.7\times$ lower. The vanilla vLLM suffers from high recomputation waste and delays in scheduling API-returned requests per FCFS policy. Delayed execution greatly impacts vanilla vLLM’s number of requests finished per second.

ImprovedDiscard maintains an API request’s original arrival time. Thus, both its normalized latency and finished requests per second are better than vanilla vLLM. However, ImprovedDiscard still incurs the same recomputation overhead and underperforms APISERVE on all metrics.

Preserve is the best among all the baselines, showing that for our mixed workload, the preserving overhead is lower than the recomputation overhead for most requests. Yet, Preserve is worse than APISERVE on all metrics.

The overall results for Swap are similar to ImprovedDiscard. Both baselines avoid GPU memory waste during API execution time. While ImprovedDiscard causes running requests to wait for the recomputation requests in an iteration, Swap causes running requests to wait for swapping out/in requests in an iteration. These overheads have similar effects on the final performance metrics.

APISERVE outperforms all of the baselines, ImprovedDiscard, Preserve, and Swap mainly because of our min-waste-based schedule. Moreover, APISERVE improves the recomputation and swap mechanisms over ImprovedDiscard and Swap with our chunking and pipelining techniques. Compared to them, APISERVE eliminates over 60% of GPU waste caused by recomputation and 96% of GPU waste for swapping.

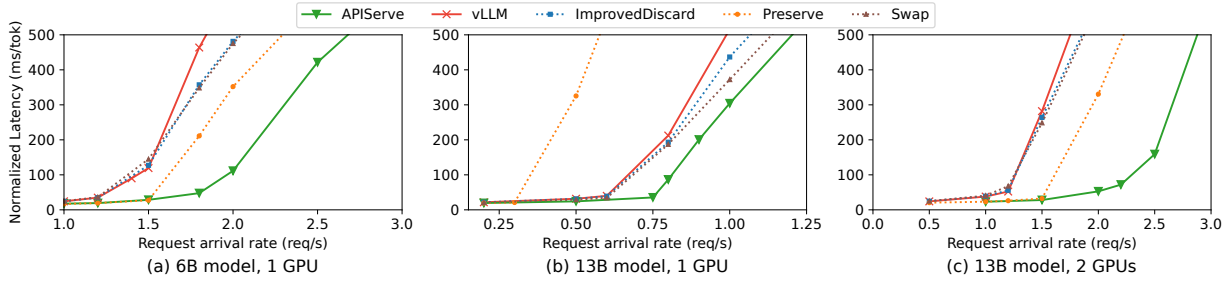


Figure 2: **Normalized Latency against Request Arrival Rate.** Lower right is better, i.e., sustains higher serving load.

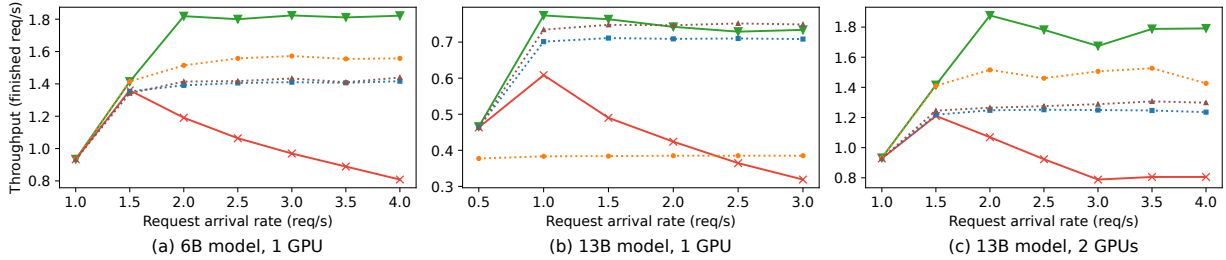


Figure 3: **Throughput against Request Arrival Rate** Throughput expressed as completed requests per second. Higher is better.

13B model results. When running the 13B model on a single GPU, APISERVE outperforms all the baselines on normalized latency but with smaller improvements than the 6B model. A larger model’s weights occupy more GPU memory, leaving less memory for KV caches. Moreover, a larger model’s normal forwarding is longer and contributes to most of the normalized latency. Thus, the room for improvement is small in general. Still, we serve up to $1.25\times$ higher request rates.

A more practical scenario for large model inference is a distributed execution environment where the model is distributed to multiple GPUs, usually with tensor parallelism (Shoeybi et al., 2020). We evaluate the 13B model on two GPUs in the same server. APISERVE outperforms all baselines by a larger margin than when running the 13B on a single GPU. APISERVE serves up to $1.8\times$ higher request arrival rates and a $1.6\times$ - $10\times$ improvement in normalized latency compared to vLLM.

Single-API workloads. Apart from the mixed workload, we evaluate APISERVE on two single-API workloads: QA and Chatbot (§2). APISERVE outperforms vLLM by up to $2.3\times$ and $1.9\times$ on normalized latency with QA and Chatbot respectively. APISERVE’s improvement with QA is larger because most QA API calls are short and have smaller waste when using preserve than discard.

5.2 Performance Deep Dive

To further understand APISERVE’s benefits, we break down its techniques by adding them one at a time to vanilla vLLM. We report the normalized latency and GPU memory waste under the load of 2 requests per second for the 6B

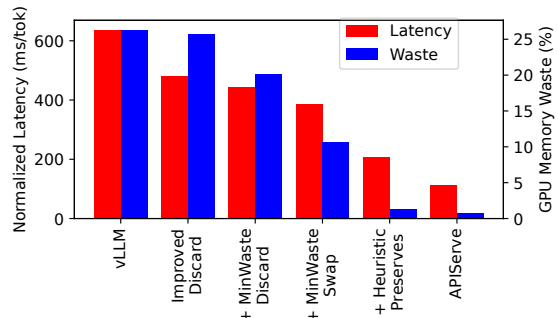


Figure 4: **APISERVE Technique Breakdown.**

model in Figure 4. Other request loads have similar trends.

We first improve Discard (vanilla vLLM) by maintaining the original API request arrival time as in ImprovedDiscard, which reduces normalized latency by 24.5%. We then add APISERVE’s recomputation chunking, resulting in 7.8% more improvement. Next, we add APISERVE’s budgeted swapping (discarding once the limit is reached). This results in an added improvement of 12.7%. Then, we add preserve and use a simple heuristic to decide between discard and preserve: discard for interactive (or long-running) APIs and preserve for automated (short-running) APIs. This addition has a 46.1% improvement, mainly because of the added support for Preserve. Finally, adding min-waste-based adaptive schedule (i.e., the whole APISERVE) results in an additional 46.4% improvement. Each of APISERVE’s techniques reduces GPU memory waste, with the whole APISERVE only having 0.69% waste. This demonstrates the effectiveness of our min-waste preemption principle.

6 Conclusion

We introduced APISERVE, an LLM inference framework optimized for API calls. By minimizing GPU memory waste as a unified objective, APISERVE delivers $1.25 \times 2 \times$ higher request arrival rates and achieves $1.6 \times 10 \times$ lower normalized latency compared to state-of-the-art inference systems.

References

- Agrawal, A., Panwar, A., Mohan, J., Kwatra, N., Gulavani, B. S., and Ramjee, R. Sarathi: Efficient llm inference by piggybacking decodes with chunked prefills. *arXiv preprint arXiv:2308.16369*, 2023.
- AI, S. Bark: Text-to-speech model. <https://github.com/suno-ai/bark>, 2023.
- Aminabadi, R. Y., Rajbhandari, S., Awan, A. A., Li, C., Li, D., Zheng, E., Ruwase, O., Smith, S., Zhang, M., Rasley, J., et al. Deepspeed-inference: enabling efficient inference of transformer models at unprecedented scale. In *SC22: International Conference for High Performance Computing, Networking, Storage and Analysis*, pp. 1–15. IEEE, 2022.
- Baeza-Yates, R., Ribeiro-Neto, B., et al. *Modern Information Retrieval*, volume 463. ACM Press, New York, 1999.
- Brockman, G., Eleti, A., Georges, E., Jang, J., Kilpatrick, L., Lim, R., Miller, L., and Pokrass, M. Introducing chatgpt and whisper apis. OpenAI Blog, March 1 2023. URL <https://openai.com/blog/introducing-chatgpt-and-whisper-apis>.
- Brysbart, M. How many words do we read per minute? a review and meta-analysis of reading rate, Apr 2019. URL osf.io/preprints/psyarxiv/xynwg.
- Chase, H. LangChain, October 2022. URL <https://github.com/langchain-ai/langchain>.
- Chiang, W.-L., Li, Z., Lin, Z., Sheng, Y., Wu, Z., Zhang, H., Zheng, L., Zhuang, S., Zhuang, Y., Gonzalez, J. E., Stoica, I., and Xing, E. P. Vicuna: An open-source chatbot impressing gpt-4 with 90%* chatgpt quality, March 2023. URL <https://lmsys.org/blog/2023-03-30-vicuna/>.
- Costa-jussà, M. R., Cross, J., Çelebi, O., Elbayad, M., Heafield, K., Heffernan, K., Kalbassi, E., Lam, J., Licht, D., Maillard, J., Sun, A., Wang, S., Wenzek, G., Youngblood, A., Akula, B., Barrault, L., Gonzalez, G. M., Hansanti, P., Hoffman, J., Jarrett, S., Sadagopan, K. R., Rowe, D., Spruit, S., Tran, C., Andrews, P., Ayan, N. F., Bhosale, S., Edunov, S., Fan, A., Gao, C., Goswami, V., Guzmán, F., Koehn, P., Mourachko, A., Ropers, C., Saleem, S., Schwenk, H., and Wang, J. No language left behind: Scaling human-centered machine translation, 2022.
- Greyling, C. When using the chatgpt api, users will have to manage the context. Medium, March 6 2023. URL <https://cobusgreyling.medium.com/when-using-the-chatgpt-api-users-will-have-to-manage-the-context-ba5869238913>.
- Gu, J., Stefani, E., Wu, Q., Thomason, J., and Wang, X. Vision-and-language navigation: A survey of tasks, methods, and future directions. In *Proceedings of the 60th Annual Meeting of the Association for Computational Linguistics (Volume 1: Long Papers)*. Association for Computational Linguistics, 2022. doi: 10.18653/v1/2022.acl-long.524. URL <http://dx.doi.org/10.18653/v1/2022.acl-long.524>.
- Hao, S., Liu, T., Wang, Z., and Hu, Z. Toolkengpt: Augmenting frozen language models with massive tools via tool embeddings. *arXiv preprint arXiv:2305.11554*, 2023.
- Hu, Y., Lin, F., Zhang, T., Yi, L., and Gao, Y. Look before you leap: Unveiling the power of gpt-4v in robotic vision-language planning, 2023.
- Huang, W., Abbeel, P., Pathak, D., and Mordatch, I. Language models as zero-shot planners: Extracting actionable knowledge for embodied agents, 2022.
- Izcard, G., Lewis, P., Lomeli, M., Hosseini, L., Petroni, F., Schick, T., Dwivedi-Yu, J., Joulin, A., Riedel, S., and Grave, E. Atlas: Few-shot learning with retrieval augmented language models, 2022.
- Kwon, W., Li, Z., Zhuang, S., Sheng, Y., Zheng, L., Yu, C. H., Gonzalez, J., Zhang, H., and Stoica, I. Efficient memory management for large language model serving with pagedattention. In *Proceedings of the 29th Symposium on Operating Systems Principles*, pp. 611–626, 2023.
- Li, Z., Zheng, L., Zhong, Y., Liu, V., Sheng, Y., Jin, X., Huang, Y., Chen, Z., Zhang, H., Gonzalez, J. E., et al. Alpaserve: Statistical multiplexing with model parallelism for deep learning serving. *arXiv preprint arXiv:2302.11665*, 2023.
- Ma, Z., Edge, D., Findlater, L., and Tan, H. Z. Haptic keyclick feedback improves typing speed and reduces typing errors on a flat keyboard. In *2015 IEEE World Haptics Conference (WHC)*, pp. 220–227. IEEE, 2015.

- Mialon, G., Dessì, R., Lomeli, M., Nalmpantis, C., Pansunuru, R., Raileanu, R., Rozière, B., Schick, T., Dwivedi-Yu, J., Celikyilmaz, A., Grave, E., LeCun, Y., and Scialom, T. Augmented language models: a survey, 2023.
- NVIDIA. Fastertransformer. <https://github.com/NVIDIA/FasterTransformer>, 2023.
- OpenAI. ChatGPT plugins. <https://openai.com/blog/chatgpt-plugins>, March 2023.
- OpenAI, :, Achiam, J., Adler, S., Agarwal, S., Ahmad, L., Akkaya, I., Aleman, F. L., Almeida, D., Altenschmidt, J., Altman, S., Anadkat, S., Avila, R., Babuschkin, I., Balaji, S., Balcom, V., Baltescu, P., Bao, H., Bavarian, M., Belgum, J., Bello, I., Berdine, J., Bernadett-Shapiro, G., Berner, C., Bogdonoff, L., Boiko, O., Boyd, M., Brakman, A.-L., Brockman, G., Brooks, T., Brundage, M., Button, K., Cai, T., Campbell, R., Cann, A., Carey, B., Carlson, C., Carmichael, R., Chan, B., Chang, C., Chantzis, F., Chen, D., Chen, S., Chen, R., Chen, J., Chen, M., Chess, B., Cho, C., Chu, C., Chung, H. W., Cummings, D., Currier, J., Dai, Y., Decareaux, C., Degry, T., Deutsch, N., Deville, D., Dhar, A., Dohan, D., Dowling, S., Dunning, S., Ecoffet, A., Eleti, A., Eloundou, T., Farhi, D., Fedus, L., Felix, N., Fishman, S. P., Forte, J., Fulford, I., Gao, L., Georges, E., Gibson, C., Goel, V., Gogineni, T., Goh, G., Gontijo-Lopes, R., Gordon, J., Grafstein, M., Gray, S., Greene, R., Gross, J., Gu, S. S., Guo, Y., Hallacy, C., Han, J., Harris, J., He, Y., Heaton, M., Heidecke, J., Hesse, C., Hickey, A., Hickey, W., Hoeschele, P., Houghton, B., Hsu, K., Hu, S., Hu, X., Huizinga, J., Jain, S., Jain, S., Jang, J., Jiang, A., Jiang, R., Jin, H., Jin, D., Jomoto, S., Jonn, B., Jun, H., Kaftan, T., Łukasz Kaiser, Kamali, A., Kanitscheider, I., Keskar, N. S., Khan, T., Kilpatrick, L., Kim, J. W., Kim, C., Kim, Y., Kirchner, H., Kiros, J., Knight, M., Kokotajlo, D., Łukasz Kondraciuk, Kondrich, A., Konstantinidis, A., Kosic, K., Krueger, G., Kuo, V., Lampe, M., Lan, I., Lee, T., Leike, J., Leung, J., Levy, D., Li, C. M., Lim, R., Lin, M., Lin, S., Litwin, M., Lopez, T., Lowe, R., Lue, P., Makanju, A., Malfacini, K., Manning, S., Markov, T., Markovski, Y., Martin, B., Mayer, K., Mayne, A., McGrew, B., McKinney, S. M., McLeavey, C., McMillan, P., McNeil, J., Medina, D., Mehta, A., Menick, J., Metz, L., Mishchenko, A., Mishkin, P., Monaco, V., Morikawa, E., Mossing, D., Mu, T., Murati, M., Murk, O., Mély, D., Nair, A., Nakano, R., Nayak, R., Neelakantan, A., Ngo, R., Noh, H., Ouyang, L., O’Keefe, C., Pachocki, J., Paino, A., Palermo, J., Pantuliano, A., Parascandolo, G., Parish, J., Parparita, E., Passos, A., Pavlov, M., Peng, A., Perelman, A., de Avila Belbute Peres, F., Petrov, M., de Oliveira Pinto, H. P., Michael, Pokorny, Pokrass, M., Pong, V., Powell, T., Power, A., Power, B., Proehl, E., Puri, R., Radford, A., Rae, J., Ramesh, A., Raymond, C., Real, F., Rimbach, K., Ross, C., Rotsted, B., Roussez, H., Ryder, N., Saltarelli, M., Sanders, T., Santurkar, S., Sastry, G., Schmidt, H., Schnurr, D., Schulman, J., Sel-sam, D., Sheppard, K., Sherbakov, T., Shieh, J., Shoker, S., Shyam, P., Sidor, S., Sigler, E., Simens, M., Sitkin, J., Slama, K., Sohl, I., Sokolowsky, B., Song, Y., Staudacher, N., Such, F. P., Summers, N., Sutskever, I., Tang, J., Tezak, N., Thompson, M., Tillet, P., Tootoonchian, A., Tseng, E., Tuggle, P., Turley, N., Tworek, J., Uribe, J. F. C., Vallone, A., Vijayvergiya, A., Voss, C., Wainwright, C., Wang, J. J., Wang, A., Wang, B., Ward, J., Wei, J., Weinmann, C., Welihinda, A., Welinder, P., Weng, J., Weng, L., Wiethoff, M., Willner, D., Winter, C., Wolrich, S., Wong, H., Workman, L., Wu, S., Wu, J., Wu, M., Xiao, K., Xu, T., Yoo, S., Yu, K., Yuan, Q., Zaremba, W., Zellers, R., Zhang, C., Zhang, M., Zhao, S., Zheng, T., Zhuang, J., Zhuk, W., and Zoph, B. Gpt-4 technical report, 2023.
- OpenTable. New: Chatgpt restaurant recs, powered by opentable, March 23 2023. URL <https://www.opentable.com/blog/chatgpt/>.
- Parisi, A., Zhao, Y., and Fiedel, N. Talm: Tool augmented language models. *arXiv preprint arXiv:2205.12255*, 2022.
- Patil, S. G., Zhang, T., Wang, X., and Gonzalez, J. E. Gorilla: Large language model connected with massive apis. *arXiv preprint arXiv:2305.15334*, 2023.
- Rombach, R., Blattmann, A., Lorenz, D., Esser, P., and Ommer, B. High-resolution image synthesis with latent diffusion models, 2021.
- Schick, T., Dwivedi-Yu, J., Dessì, R., Raileanu, R., Lomeli, M., Zettlemoyer, L., Cancedda, N., and Scialom, T. Toolformer: Language models can teach themselves to use tools. *arXiv preprint arXiv:2302.04761*, 2023.
- Shoeybi, M., Patwary, M., Puri, R., LeGresley, P., Casper, J., and Catanzaro, B. Megatron-lm: Training multi-billion parameter language models using model parallelism, 2020.
- Shridhar, M., Yuan, X., Côté, M.-A., Bisk, Y., Trischler, A., and Hausknecht, M. Alfworld: Aligning text and embodied environments for interactive learning. *arXiv preprint arXiv:2010.03768*, 2020.
- Touvron, H., Lavril, T., Izacard, G., Martinet, X., Lachaux, M.-A., Lacroix, T., Rozière, B., Goyal, N., Hambro, E., Azhar, F., et al. Llama: Open and efficient foundation language models. *arXiv preprint arXiv:2302.13971*, 2023.

- Wang, B. and Komatsuzaki, A. GPT-J-6B: A 6 Billion Parameter Autoregressive Language Model. <https://github.com/kingoflolz/mesh-transformer-jax>, May 2021.
- Wei, J., Wang, X., Schuurmans, D., Bosma, M., Xia, F., Chi, E., Le, Q. V., Zhou, D., et al. Chain-of-thought prompting elicits reasoning in large language models. *Advances in Neural Information Processing Systems*, 35: 24824–24837, 2022.
- Wolfram, S. Chatgpt gets its 'wolfram superpowers'! Stephen Wolfram Writings, 2023. URL <https://writings.stephenwolfram.com/2023/03/chatgpt-gets-its-wolfram-superpowers/>.
- Wu, B., Zhong, Y., Zhang, Z., Huang, G., Liu, X., and Jin, X. Fast distributed inference serving for large language models, 2023.
- Yang, Z., Qi, P., Zhang, S., Bengio, Y., Cohen, W. W., Salakhutdinov, R., and Manning, C. D. Hotpotqa: A dataset for diverse, explainable multi-hop question answering. *arXiv preprint arXiv:1809.09600*, 2018.
- Yao, S., Zhao, J., Yu, D., Du, N., Shafran, I., Narasimhan, K., and Cao, Y. React: Synergizing reasoning and acting in language models. *arXiv preprint arXiv:2210.03629*, 2022.
- Yu, G.-I., Jeong, J. S., Kim, G.-W., Kim, S., and Chun, B.-G. Orca: A Distributed Serving System for Transformer-Based Generative Models. In *16th USENIX Symposium on Operating Systems Design and Implementation (OSDI '22)*, Carlsbad, CA, July 2022.
- Zhang, Z., Zhang, A., Li, M., and Smola, A. Automatic chain of thought prompting in large language models, 2022.
- Zheng, L., Chiang, W.-L., Sheng, Y., Zhuang, S., Wu, Z., Zhuang, Y., Lin, Z., Li, Z., Li, D., Xing, E. P., Zhang, H., Gonzalez, J. E., and Stoica, I. Judging llm-as-a-judge with mt-bench and chatbot arena, 2023a.
- Zheng, L., Yin, L., Xie, Z., Huang, J., Sun, C., Yu, C. H., Cao, S., Kozyrakis, C., Stoica, I., Gonzalez, J. E., Barrett, C., and Sheng, Y. Efficiently programming large language models using slang, 2023b.
- Zhong, Y., Liu, S., Chen, J., Hu, J., Zhu, Y., Liu, X., Jin, X., and Zhang, H. Distserve: Disaggregating prefill and decoding for goodput-optimized large language model serving, 2024.

Appendix

API Properties and Dataset Generation

We analyze the properties of different datasets to evaluate the effectiveness of our inference system. We consider datasets from arithmetic, a knowledge-based question and answering system, a multi-step chat bot, and an embodied virtual environment. The dataset demonstrates different execution time, frequency of API calls, and context lengths. We augment the datasets with relevant APIs from calculator, wikipedia, and a virtual environment gym.

We measure the API execution time, the number of API calls, the number of returned tokens of an API call, and the context length when an API is called. Figures 5 and 6 present the detailed CDF results the four metrics for short-running APIs (math, QA, VE) and long-running APIs (chatbot, image, TTS). Below, we briefly introduce each API type and discuss their properties.

We use the ReAct framework to prompt the LLM to call a Wikipedia endpoint with different questions. The responses from the Wikipedia endpoint are postprocessed. We use the live Wikipedia API endpoint for our benchmark and for each call, we retrieve a summary of the relevant Wikipedia page, which we post-process by limiting the size of the responses to fit within the maximum model sequence length.

To evaluate VE, we prompt GPT-4 LLM with an initial virtual environment and use the ReAct event loop to repeatedly interact with the environment. For our evaluation, we truncate to fit within the context length.

We prompt GPT-4 to generate complex Stable Diffusion prompts at a certain size. Each prompt will trigger an API call of the Stable Diffusion model (Rombach et al., 2021) to generate an image. Each round with the LLM involves a user prompt with normal decoding and then a diffusion call. The number of calls total is modeled around the chat dataset. We estimate the number of image generation rounds (*i.e.*, number of API calls) to be the same as the number of chatting rounds in Chatbot. As there is no standard way of returning tokens from an image generation, we use a short, constant-length sentence describing the generated image as returned tokens. For API execution time, we measure the actual Stable Diffusion call and estimate the human response time in the same as Chatbot; the sum of them at each round is shown in Table 1 and Figure 6. For the context and return length, we provide a mixture of ShareGPT dataset (Zheng et al., 2023a) and the real prompts.

We use a methodology similar to image generation to un-

derstand TTS-augmented LLMs.

Implementation Details

We implement APISERVE on top of vLLM and build APISERVE, an inference system designed for API-augmented LLMs. As shown in Figure 8, APISERVE includes an API executor that performs different API calls, an iterative-level scheduler that forms a batch of waiting requests and (partial) paused requests, a swap manager that facilitates GPU/CPU memory swapping, a running status monitor that monitors the resource usage and size of running requests, a waste estimator that calculates GPU memory waste for each API-paused request, and an offline profiler that collects basic systems metrics before starting serving.

At the end of each iteration, the scheduler gathers all requests that trigger API calls, adds them to the paused-request queue, swaps as much context (computed keys and values) of paused requests as allowed to CPU memory, determines whether to preserve or discard the remaining context of each paused request based on the GPU memory waste amount calculated by the waste estimator, and calls the actual API. When an API call finishes, APISERVE determines how many swapped-out or discarded tokens to swap in or recompute in the next iteration. It also determines how many waiting requests (non-API paused requests) to schedule in the next iteration. When all the context of a paused request has been restored, APISERVE adds the tokens returned by the API call to the resumed request.

Additional Evaluation Results

A major distinction between typical inference workloads and tool-augmented workloads is the added latency from API execution. We observe that 31% percent of the median request end-to-end time is spent waiting on its API to return. This means requests take longer to complete, which can add significant latency for those in the waiting queue. Hence, we place an emphasis on improving time to first token (TTFT) in addition to improving serving throughput as measured by vLLM and Orca. We vary request arrival rate and collect median TTFT as well as median normalized end-to-end latency. Normalized latency is measured by dividing the request end-to-end time by its output length. In our metric, we remove a request’s API execution time from its end-to-end latency because the user perceives the API execution, which means the system is not penalized. All experiments use 30-minute traces. The results on our 6B,

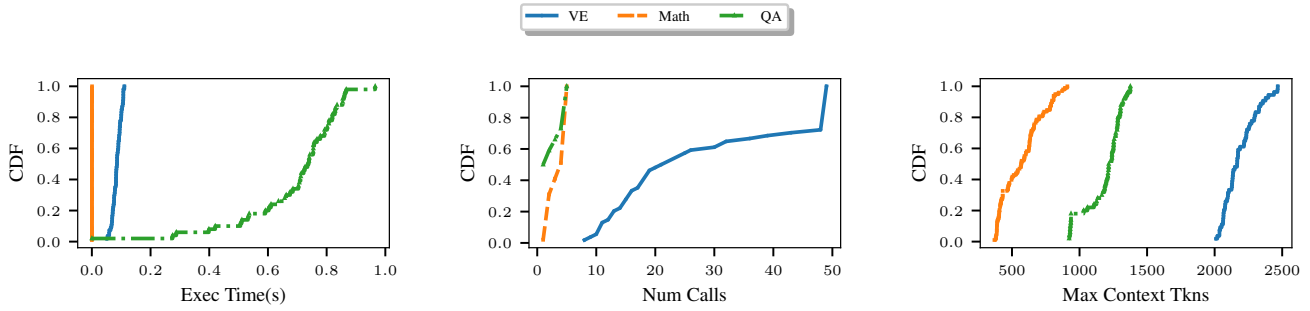


Figure 5: **CDF Results of Short APIs.** Each line plots the CDF distribution of all the calls of one API type.

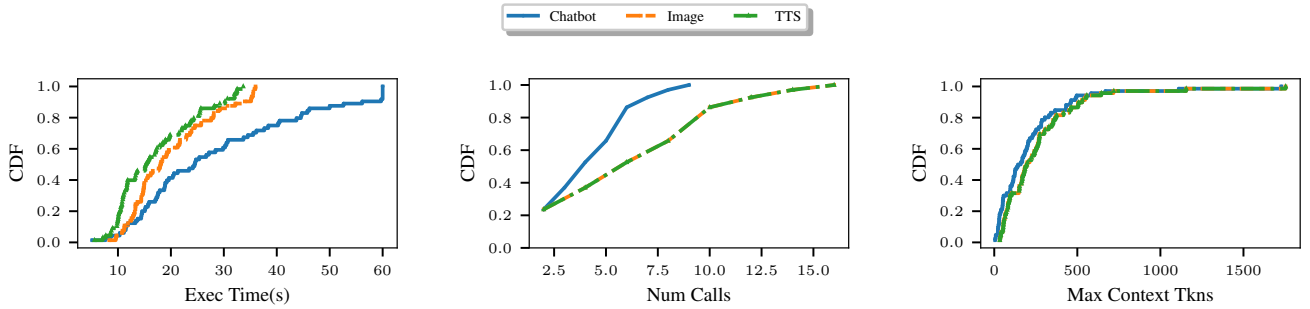


Figure 6: **CDF Results of Long APIs.** Each line plots the CDF distribution of all the calls of one API type.

13B, and distributed 13B models are shown in Figure 7.

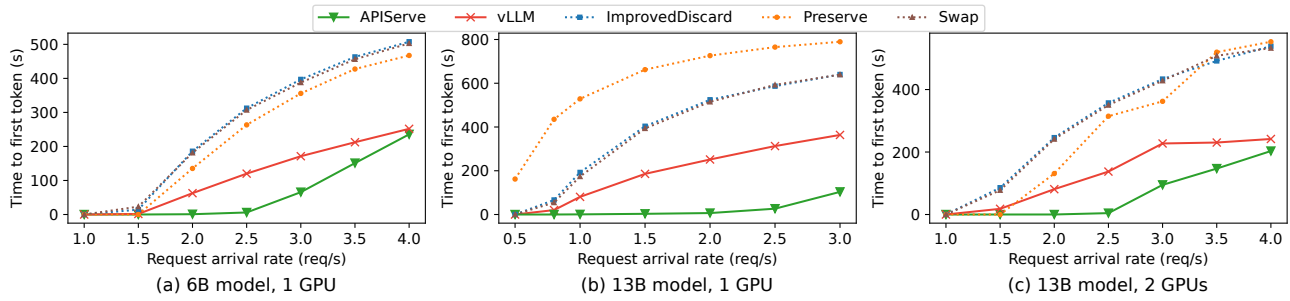


Figure 7: Time-to-first-token (TTFT) with 6B and 13B models on the mixed workload

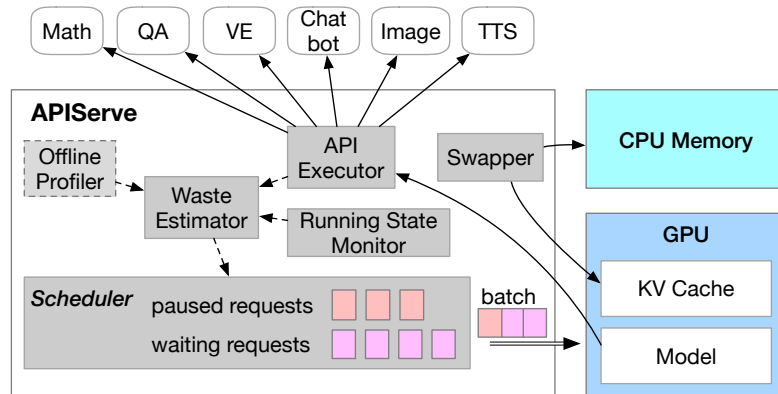


Figure 8: Overall APISERVE Architecture.